Arriving at an Experimental Estimate of the Intrinsic Activation Barrier of Olefin Insertion into the Zr−C Bond of an Active Metallocene Ziegler Catalyst

Jörn Karl, Marc Dahlmann, Gerhard Erker,* and Klaus Bergander

Contribution from the Organisch-Chemisches Institut der Universität Münster, Corrensstrasse 40, D-48149 Münster, Germany

Received December 29, 1997

Abstract: Bis(η-methylcyclopentadienyl)(η^4-butadiene)zirconium adds 1 equiv of the organometallic Lewis acid $B(C_6F_5)_3$ to yield the metallocene−(μ-C_4H_6)−borate betaine **5**, which is an active, homogeneous, one-component Ziegler catalyst for the polymerization of 1-alkenes. The metallacyclic metallocene betaine **5** undergoes a degenerate $\pi \rightleftharpoons \sigma \rightleftharpoons \pi$-allyl interconversion on the NMR time scale in toluene solution ($\Delta G^{\ddagger}_{m(obs)}$-(toluene) = 19.8 kcal mol^{-1}) which becomes markedly faster in the presence of added reactive 1-alkenes ($\Delta G^{\ddagger}_{m(obs)}$ = 18.9 (1-hexene), 17.7 (1-pentene), 17.5 (1-butene), 17.2 kcal mol^{-1} (propene)). This lowering of the activation barrier is probably due to an increased stabilization of the (σ-alkyl)(π-alkene)metallocene betaine intermediate **7**, which at the same time is passed as the essential intermediate stage of the insertion of these alkenes into the reactive zirconium carbon bond of **5** to yield the mono olefin insertion products **9**. The Gibbs activation energies of this chemical insertion reaction ($\Delta G^{\ddagger}_{chem}$ = 20.1 (1-hexene), 18.8 (1-pentene), 18.5 (1-butene), 17.3 kcal mol^{-1} (propene)) are similar in magnitude to the activation energies of magnetical exchange ($\Delta G^{\ddagger}_{m(obs)}$). This creates the interesting situation that in the presence of these reactive 1-alkenes, the (reversible) magnetical exchange rate ($k_{m(obs)}$), as determined by the dynamic NMR experiment, is dependent on the rate of the competing (irreversible) overall chemical addition reaction (k_{chem}). The rate constants $k_{m(obs)}$ and k_{chem} were measured in the presence of these 1-alkenes, which allowed for a determination of the height of the first, i.e., the complexation barrier ($\Delta G^{\ddagger}_1$ = 18.5 (1-hexene), 17.3 (1-pentene), 17.1 (1-butene), 16.4 kcal mol^{-1} (propene); standard state $c^{\ominus}$ = 1 mol L^{-1}) and its difference ($\Delta\Delta G^{\ddagger}_2$) to the top of the actual insertion barrier ($\Delta\Delta G^{\ddagger}_2$ = 1.6 (1-hexene), 1.5 (1-pentene), 1.3 (1-butene), 0.7 kcal mol^{-1} (propene)). These values, together with the activation energy of the degenerate allyl ligand interconversion of the model system (σ-allyl)(π-allyl)zirconocene (**10**) ($\Delta G^{\ddagger}_3$ = 7 ± 0.5 kcal mol^{-1}), allowed for a good experimentally based estimate of the intrinsic activation energy (reaction **7** → **9**) of the insertion of these 1-alkenes into the zirconium carbon bond at this group 4 bent metallocene unit. The thus obtained insertion barrier is $\Delta G^{\ddagger}_{ins} \approx 10-11$ kcal mol^{-1} for the 1-alkenes used in this study. The alkene decomplexation barrier (reaction **7** → **5**) is lower by ca. 1−2 kcal mol^{-1}.

Introduction

Group 4 metallocene-derived homogeneous Ziegler catalysts have become of enormous importance in olefin polymerization chemistry.[1] The active catalyst systems are readily generated in situ from $(^{R}Cp)_2ZrR_2$ or $(^{R}Cp)_2ZrX_2$ precursors by treatment with a variety of activator compounds (e.g., methylalumoxane, $B(C_6F_5)_3$, carbenium ions, or Brönstedt acids associated with anions of very low nucleophilicities).[2] It is well accepted that the active chain-propagating metal species is of an alkylzirconocene cation type,[3] probably involving some stabilizing agostic C−H···Zr interaction. The CC coupling catalytic process in most cases is characterized by very high reaction rates; corresponding overall (standard state) Gibbs activation barriers of $\Delta G^{\ddagger} \approx 15 \pm 3$ kcal/mol are not all uncommon.[1b]

Many details of the mechanistic scheme that leads to incorporation of the added α-olefin molecule into the growing polymer chain appear to be reasonably well understood.[1] We know about the stereochemical role of the metallocene backbone[4] and also of cases where the polymer chain end must serve as an additional relay to transfer the stereochemical features of the metallocene backbone onto the growing carbon chain.[5] But we have a limited knowledge concerning the quantitative description of the hypersurface of the repetitive step of the catalytic cycle (see Scheme 1). It can be assumed that it starts from a very reactive alkyl zirconocene cation (**1**), probably

* E-mail: erker@uni-muenster.de. Fax: +49(0)251-83 36503.

(1) (a) Aulbach, M.; Küber, F. *Chem. Unserer Zeit* **1994**, *28*, 197. (b) Brintzinger, H.-H.; Fischer, D.; Mülhaupt, R.; Rieger, B.; Waymouth, R. *Angew. Chem.* **1995**, *107*, 1255; *Angew. Chem., Int. Ed. Engl.* **1995**, *34*, 1143 and references cited therein.

(2) (a) Sinn, H.; Kaminsky, W. *Adv. Organomet. Chem.* **1980**, *18*, 99. (b) Bochmann, M.; Jaggar, A. J.; Nicholls, J. C. *Angew. Chem.* **1990**, *102*, 830; *Angew. Chem., Int. Ed. Engl.* **1990**, *29*, 780. Bochmann, M. *J. Chem. Soc., Dalton Trans.* **1996**, 255 and references cited therein. See also: (c) Chien, J. C. W.; Tsai, W.-M.; Rausch, M. D. *J. Am. Chem. Soc.* **1991**, *113*, 8570. (d) Yang, X.; Stern, C. L.; Marks, T. J. *J. Am. Chem. Soc.* **1994**, *116*, 10015.

(3) Jordan, R. F. *Adv. Organomet. Chem.* **1991**, *32*, 325.

(4) Ewen, J. A. *J. Am. Chem. Soc.* **1984**, *106*, 6355. Kaminsky, W.; Külper, K.; Brintzinger, H.-H.; Wild, F. R. W. P. *Angew. Chem.* **1985**, *97*, 507; *Angew. Chem., Int. Ed. Engl.* **1985**, *24*, 507. Spaleck, W.; Antberg, M.; Rohrmann, J.; Winter, A.; Bachmann, B.; Kiprof, P.; Behm, J.; Herrmann, W. A. *Angew. Chem.* **1992**, *104*, 1373; *Angew. Chem., Int. Ed. Engl.* **1992**, *31*, 1347. Ewen, J. A.; Jones, L. A.; Razavi, A.; Ferrara, J. D. *J. Am. Chem. Soc.* **1988**, *110*, 6255. Könemann, M.; Erker, G.; Fröhlich, R.; Kotila, S. *Organometallics* **1997**, *16*, 2900.

S0002-7863(97)04380-1 CCC: $15.00
Published on Web 05/30/1998

Scheme 1

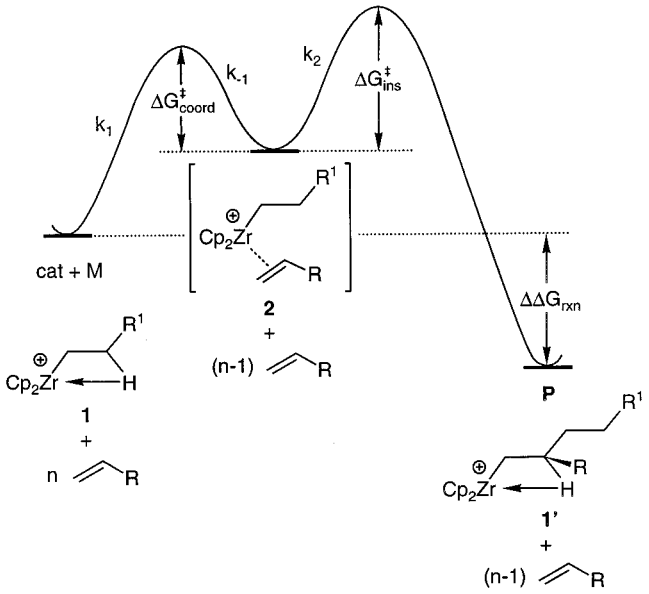

internally stabilized by an agostic C−H···M interaction,[6] which adds an alkene to form the reactive intermediate **2**. This then undergoes the insertion reaction which leads to carbon−carbon coupling, very exothermically ($\Delta\Delta G_{rxn} \approx 20$ kcal/mol), of course, because a new C−C single bond is formed at the expense of the π-component of the C=C double bond of the monomer. This sequence is followed time and again until a chain-transfer reaction takes place.[7]

It is tempting to assume that the dominating stereocontrol of the overall process is governed by the first step, the addition of the metallocene to the *Re* or *Si* face of the 1-alkene, and many studies seem to have quietly implied this interpretation without explicitly stating it.[1,4]

But from the overall reaction scheme (see Scheme 1), it is quite obvious that one cannot *a priori* derive at this conclusion without knowing about the relative height of the second activation barrier, i.e., the intrinsic alkene insertion barrier of the metallocene catalyst system. Only if this second barrier (rate constant k_2, insertion barrier $\Delta G^{\ddagger}_{ins}$) is rather low can overcoming the first barrier (rate constants k_1 and k_{-1}, complexation barrier $\Delta G^{\ddagger}_1$) become rate and selectivity determining. But it is well conceivable that the second barrier is of a substantial height and may, therefore, help to determine the selectivity properties of the whole system or even, in some cases, dominate it. In this respect, it is very likely that metallocenes may kinetically exhibit an enzyme-like behavior. In enzyme catalysis, it is well-known that in a quite analogous kinetic situation, either of the two scenarios—rate and product properties determination of either the first or second step—is known, and there have even been examples of a switchover from the dominating first step to second step control being observed in a series of enzymatically catalyzed reactions just by altering the substrate.[8]

Since the overall kinetic expressions of metallocene and enzymatic catalysis are alike (as shown in eq 1 using the *k* values as defined in Scheme 1), a similar behavior of these very

$$\frac{dP}{dt} = k_2 \frac{k_1}{k_{-1} + k_2}[\text{catalyst}][\text{monomer}] = \frac{k_2}{K_m}[\text{cat}][\text{M}] \quad (1)$$

different types of catalysts is likely, and one needs to know the actual magnitude of the alkene insertion activation barrier ($\Delta G^{\ddagger}_{ins}$) of a given metallocene catalyst system to understand its preferred way of controlling the selectivity of catalytic polymer formation.

This question had been addressed repeatedly by computational chemistry, initially with conflicting results[9] but lately with an emerging picture of congruence, where more sophisticated theoretical methods have been used.[10] Whereas predictions of very low insertion barriers ($\Delta G^{\ddagger}_{ins}$) seemed to prevail in the early studies, current calculations appear to focus on values of $\Delta G^{\ddagger}_{ins}$ around ca. 7−10 kcal/mol. We felt that is was a timely task to address the question of determining the $\Delta G^{\ddagger}_{ins}$ barrier of a metallocene Ziegler catalyst system experimentally. Using the actual intermediate (**2**) of the repetitive catalytic, for example, ethene or propene polymerization reaction seems not to be feasible directly at present due to its extremely high reactivity and its fleeting kinetic nature. We had to make use of a specific example out of the small number of existing realistic model systems of the metallocene Ziegler process,[11] by selecting a system that is characterized by making a brief stop on the way to forming the polymer chain after a singular

(5) (a) Longo, P.; Grassi, A.; Pellecchia, P.; Zambelli, A. *Macromolecules* **1987**, *20*, 1015. Zambelli, A.; Pellecchia, C.; Oliva, L. *Makromol. Chem., Macromol. Symp.* **1991**, *48/49*, 297. Sacchi, M. C.; Barsties, E.; Tritto, I.; Locatelli, P.; Brintzinger, H.-H.; Stehling, U. *Macromolecules* **1997**, *30*, 3955. (b) Erker, G.; Nolte, R.; Tsay, Y.-H.; Krüger, C. *Angew. Chem.* **1989**, *101*, 642; *Angew. Chem. Int. Ed. Engl.* **1989**, *28*, 628. (c) Corradini, P. *Makromol. Chem., Macromol. Symp.* **1993**, *66*, 11. Busico, V.; Cipullo, R.; Chadwick, J. C.; Modder, J. F.; Sudmeijer, O. *Macromolecules* **1994**, *27*, 7538. Guerra, G.; Cavallo, L.; Moscardi, G.; Vacatello, M.; Corradini, P. *J. Am. Chem. Soc.* **1994**, *116*, 2988. Busico, V.; Cipullo, R. *J. Am. Chem. Soc.* **1994**, *116*, 9329. Carvill, A.; Tritto, I.; Locatelli, P.; Sacchi, M. C. *Macromolecules* **1997**, *30*, 7056. Guerra, G.; Longo, P.; Cavallo, L.; Corradini, P.; Resconi, L. *J. Am. Chem. Soc.* **1997**, *119*, 4394. van der Leek, Y.; Angermund, K.; Reffke, M.; Kleinschmidt, R.; Goretzki, R.; Fink, G. *Chem. Eur. J.* **1997**, *3*, 585.

(6) (a) Ivin, K. J.; Rooney, J. J.; Stewart, C. D.; Green, M. L. H.; Mahtab, R. *J. Chem. Soc., Chem. Commun.* **1978**, 604. Green, M. L. H. *Pure Appl. Chem.* **1978**, *50*, 27. Laverty, D. T.; Rooney, J. J. *J. Chem. Soc., Faraday Trans. 1* **1983**, *79*, 869. Brookhart, M.; Green, M. L. H. *J. Organomet. Chem.* **1983**, *250*, 395. Brookhart, M.; Green, M. L. H.; Pardy, R. B. A. *J. Chem. Soc., Chem. Commun.* **1983**, 691. (b) Clawson, L.; Soto, J.; Buchwald, S. L.; Steigerwald, M. L.; Grubbs, R. H. *J. Am. Chem. Soc.* **1985**, *107*, 3377. Piers, W. E.; Bercaw, J. E. *J. Am. Chem. Soc.* **1990**, *112*, 9406. Kranledat, H.; Brintzinger, H.-H. *Angew. Chem.* **1990**, *102*, 1459; *Angew. Chem., Int. Ed. Engl.* **1990**, *29*, 1412. Janiak, B. *J. Organomet. Chem.* **1993**, *452*, 63. Barta, N. S.; Kirk, B. A.; Stille, J. R. *J. Am. Chem. Soc.* **1994**, *116*, 8912. Leclerc, M. K.; Brintzinger, H. H. *J. Am. Chem. Soc.* **1995**, *117*, 1651; **1996**, *118*, 9024. Prosenc, M.-H.; Brintzinger, H.-H. *Organometallics* **1997**, *16*, 3889. (c) Jordan, R. F.; Bradley, P. K.; Baenziger, N. C.; LaPointe, R. E. *J. Am. Chem. Soc.* **1990**, *112*, 1289. Alelyunas, Y. W.; Guo, Z.; LaPointe, R. E.; Jordan, R. F. *Organometallics* **1993**, *12*, 544. Alelyunas, Y. W.; Baenziger, N. C.; Bradley, P. K.; Jordan, R. F. *Organometallics* **1994**, *13*, 148. Guo, Z.; Swenson, D. C.; Jordan, R. F. *Organometallics* **1994**, *13*, 1424.

(7) Luinstra, G. A.; Vogelzang, J.; Teuben, J. H. *Organometallics* **1992**, *11*, 2273. Cavallo, L.; Guerra, G. *Macromolecules* **1996**, *29*, 2729. Resconi, L.; Piemontesi, F.; Franciscono, G.; Abis, L.; Fiorani, T. *J. Am. Chem. Soc.* **1992**, *114*, 1025.

(8) Walsh, C. *Enzymatic Reaction Mechanism*; Freeman: San Francisco, 1977. Bender, M.; Kezdy, F. *Annu. Rev. Biochem.* **1965**, *34*, 49.

(9) Kawamura-Kuribayashi, H.; Koga, N.; Morokuma, K. *J. Am. Chem. Soc.* **1992**, *114*, 2359. Castonguay, L. A.; Rappé, A. K. *J. Am. Chem. Soc.* **1992**, *114*, 5832. Woo, T. K.; Fan, L.; Ziegler, T. *Organometallics* **1994**, *13*, 432, 2252. Weiss, H.; Ehrig, M.; Ahlrichs, R. *J. Am. Chem. Soc.* **1994**, *116*, 4919. Meier, R. J.; van Doremaele, G. H. J.; Iarlori, S.; Buda, F. *J. Am. Chem. Soc.* **1994**, *116*, 7274; *Macromol. Symp.* **1995**, *89*, 369; *THEOCHEM* **1996**, *363*, 269. Hyla-Kryspin, I.; Niu, S.; Gleiter, R. *Organometallics* **1995**, *14*, 964. Lohrenz, J. C. W.; Woo, T. K.; Fan, L.; Ziegler, T. *J. Organomet. Chem.* **1995**, *497*, 91. Lohrenz, J. C. W.; Woo, T. K.; Ziegler, T. *J. Am. Chem. Soc.* **1995**, *117*, 12793. Fan, L.; Harrison, D.; Deng, L.; Woo, T. K.; Swerhone, D.; Ziegler, T. *Can. J. Chem.* **1995**, *73*, 989. Yoshida, T.; Koga, N.; Morokuma, K. *Organometallics* **1996**, *15*, 766. Støvneng, J. A.; Rytter, E. *J. Organomet. Chem.* **1996**, *519*, 277.

insertion step, thereby allowing us to make the necessary series of measurements that would eventually lead to a sufficiently reliable experimental estimate of the $\Delta G^{\ddagger}_{ins}$ value. Using a selected example, this was done successfully, and to the best of our knowledge, for the first time, the alkene insertion barrier ($\Delta G^{\ddagger}_{ins}$) of a metallocene Ziegler system was experimentally determined.

Results and Discussion

The system that we have used for this study is derived from (butadiene)zirconocene (**3a**).[12] As we had previously shown, this reagent cleanly adds the strong organometallic Lewis acid

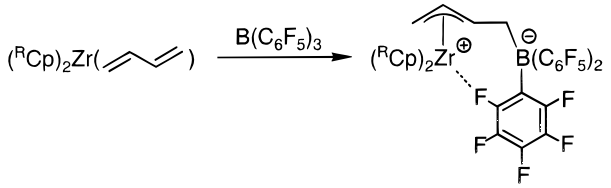

R = H, **3a**
R = CH_3, **3b**

R = H, **4**
R = CH_3, **5**

$B(C_6F_5)_3$[13] selectively at the C4 position of the conjugated diene ligand to form the distorted metallocene−borate−betaine complex **4**.[14] In **4**, the electrophilic zirconium center is protected by means of an intramolecular coordination of a single *o*-fluorine atom of the $B(C_6F_5)_3$ group. The presence of the Zr···F−C interaction was clearly shown by ^{19}F NMR spectroscopy at low temperature (single signal at δ −213 ppm, 193 K), and it is also featured in the X-ray crystal structure analysis of **4** (d(Zr···F) = 2.423(3) Å).[15] Thermodynamically, the Zr···F−C interaction is rather weak. From the dynamic ^{19}F NMR spectra, a Zr···F bond dissociation energy of ca. 8 kcal/mol was estimated. The bis(methylcyclopentadienyl)Zr(butadiene) (**3b**) derived addition product **5** that was predominantly used in this study behaves analogously.[16]

The complexes **4** and **5** exhibit the dynamic behavior of the (π-allyl)metallocene moiety. This is monitored by an intramolecular equilibration process involving the diastereotopic ^{R}Cp

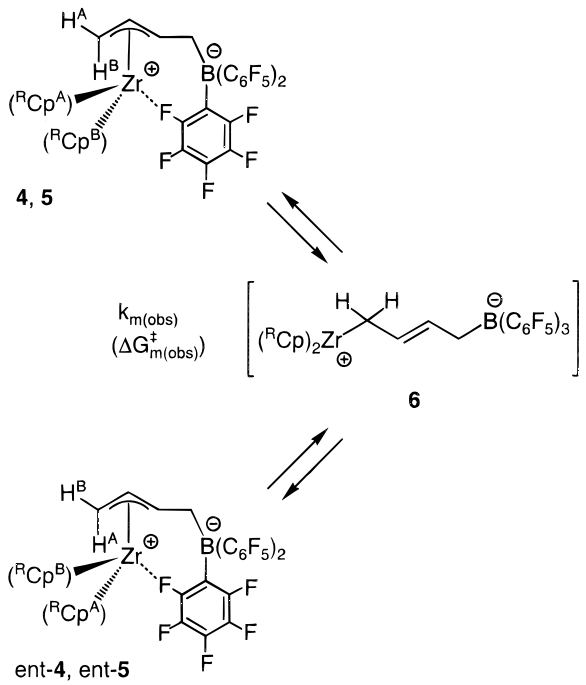

ligand systems as well as 1-H_{syn} ⇌ 1-H_{anti} exchange of proton positions at the unsubstituted η^3-allyl ligand terminus. This process is very likely proceeding through an σ-allyl-type intermediate (**6**).[17,18] We shall see later that it is probably a derivative of this intermediate, namely, a reactive corresponding (σ-allyl)(π-alkene)metallocene betaine system (**7**, see below), that is formed in the first step of the initiating reaction sequence,[19,20] ultimately leading to polymerization of the alkene.

(10) Jolly, C. A.; Marynick, D. S. *J. Am. Chem. Soc.* **1989**, *111*, 7968. Kawamura-Kuribayashi, H.; Koga, N.; Morokuma, K. *J. Am. Chem. Soc.* **1992**, *114*, 8687. Jensen, V. R.; Ystenes, M.; Wärnmark, K.; Åkermark, B.; Svensson, M.; Siegbahn, P. E. M.; Blomberg, M. R. A. *Organometallics* **1994**, *13*, 282. Bierwagen, E. P.; Bercaw, J. E.; Goddard, W. A., III *J. Am. Chem. Soc.* **1994**, *116*, 1481. Fan, L.; Harrison, D.; Woo, T. K.; Ziegler, T. *Organometallics* **1995**, *14*, 2018. Yoshida, T.; Koga, N.; Morokuma, K. *Organometallics* **1995**, *14*, 746. Jensen, V. R.; Børve, K. J.; Ystenes, M. *J. Am. Chem. Soc.* **1995**, *117*, 4109. Cruz, V. L.; Muñoz-Escalona, A.; Martinez-Salazar, J. *Polymer* **1996**, *37*, 1663. Woo, T. K.; Margl, P. M.; Lohrenz, J. C. W.; Blöchl, P. E.; Ziegler, T. *J. Am. Chem. Soc.* **1996**, *118*, 13021. Margl. P.; Lohrenz, J. C. W.; Ziegler, T.; Blöchl, P. E. *J. Am. Chem. Soc.* **1996**, *118*, 4434. Richardson, D. E.; Alameddin, N. G.; Ryan, M. F.; Hayes, T.; Eyler, J. R.; Siedle, A. R. *J. Am. Chem. Soc.* **1996**, *118*, 11244. Guerra, G.; Cavallo, L.; Moscardi, G.; Vacatello, M.; Corradini, P. *Macromolecules* **1996**, *29*, 4834. Froese, R. D. J.; Musaev, D. G.; Matsubara, T.; Morokuma, K. *J. Am. Chem. Soc.* **1997**, *119*, 7190. Jensen, V. R.; Børve, K. J. *Organometallics* **1997**, *16*, 2514.

(11) (a) For other potential model systems, see, e.g.: Horton, A. D. *Organometallics* **1992**, *11*, 3271. Mashima, K.; Fujikawa, S.; Nakamura, A. *J. Am. Chem. Soc.* **1993**, *115*, 10990. Gilchrist, J. H.; Bercaw, J. E. *J. Am. Chem. Soc.* **1996**, *118*, 12021. Pindado, G. J.; Thornton-Pett, M.; Bowkamp, M.; Meetsma, A.; Hessen, B.; Bochmann, M. *Angew. Chem.* **1997**, *109*, 2457; *Angew. Chem., Int. Ed. Engl.* **1997**, *36*, 2358. (b) For other examples of single olefin insertion, see, e.g.: Pellecchia, C.; Grassi, A.; Zambelli, A. *J. Chem. Soc., Chem. Commun.* **1993**, 947. Pellecchia, C.; Immirzi, A.; Grassi, A.; Zambelli, A. *Organometallics* **1993**, *12*, 4473. Pellecchia, C.; Grassi, A.; Immirzi, A. *J. Am. Chem. Soc.* **1993**, *115*, 1160. Pellecchia, C.; Immirzi, A.; Pappalardo, D.; Peluso, A. *Organometallics* **1994**, *13*, 3773. Pellecchia, C.; Grassi, A.; Zambelli, A. *Organometallics* **1994**, *13*, 298. Pellecchia, C.; Immirzi, A.; Zambelli, A. *J. Organomet. Chem.* **1994**, 479, *C9*. Dagorne, S.; Rodewald, S.; Jordan, R. F. *Organometallics* **1997**, *16*, 5541 and references cited therein.

(12) (a) Erker, G.; Krüger, C.; Müller, G. *Adv. Organomet. Chem.* **1985**, *24*, 1 and references cited therein. (b) Erker, G.; Wicher, J.; Engel, K.; Rosenfeldt, F.; Dietrich, W.; Krüger, C. *J. Am. Chem. Soc.* **1980**, *102*, 6344. Erker, G.; Wicher, J.; Engel, K.; Krüger, C. *Chem. Ber.* **1982**, *115*, 3300. Erker, G.; Engel, K.; Krüger, C.; Chiang, A.-P. *Chem. Ber.* **1982**, *115*, 3311. Yasuda, H.; Kajihara, Y.; Mashima, K.; Nagasuna, K.; Lee, K.; Nakamura, A. *Organometallics* **1982**, *1*, 388.

(13) Massey, A. G.; Park, A. J.; Stone, F. G. A. *Proc. Chem. Soc.* **1963**, 212. Massey, A. G.; Park, A. J. *J. Organomet. Chem.* **1964**, *2*, 245. Massey, A. G.; Park, A. J. In *Organometallic Synthesis*; King, R. B., Eisch, J. J., Eds.; Elsevier: New York, 1986; Vol. 3, p 461.

(14) Temme, B.; Erker, G.; Karl, J.; Luftmann, H.; Fröhlich, R.; Kotila, S. *Angew. Chem.* **1995**, *107*, 1867; *Angew. Chem., Int. Ed. Engl.* **1995**, *34*, 1755. Karl, J.; Erker, G.; Fröhlich, R. *J. Organomet. Chem.* **1997**, *535*, 59.

(15) See for a comparison: Thompson, J. S.; Sorrell, T.; Marks, T. J.; Ibers, J. A. *J. Am. Chem. Soc.* **1979**, *101*, 4193. Murray-Rust, P. W.; Stallins, W. C.; Monti, C. T.; Preston, R. K.; Glusker, J. P. *J. Am. Chem. Soc.* **1983**, *105*, 3206. Catala, R. M.; Cruz-Garritz, D.; Hills, A.; Hughes, D. L.; Richards, R. L.; Sosa, P.; Torrens, H. *J. Chem. Soc., Chem. Commun.* **1987**, 261. Lin, Z.; LeMarechal, J.-F.; Sabat, M.; Marks, T. J. *J. Am. Chem. Soc.* **1987**, *109*, 4127. Stalke, D.; Whitmire, K. H. *J. Chem. Soc., Chem. Commun.* **1990**, 833. Yang, X.; Stern, C. L.; Marks, T. J. *Organometallics* **1991**, *10*, 840. Horton, A. D.; Orpen, A. G. *Organometallics* **1991**, *10*, 3910. Siedle, A. R.; Newmark, R. A.; Lamanna, W. M.; Huffman, J. C. *Organometallics* **1993**, *12*, 1491. Ruwwe, J.; Erker, G.; Fröhlich, R. *Angew. Chem.* **1996**, *108*, 108; *Angew. Chem., Int. Ed. Engl.* **1996**, *35*, 80. Plenio, H.; Diodone, R. *Chem. Ber.* **1996**, *129*, 1211. Plenio, H.; Diodone, R.; Badura, D. *Angew. Chem.* **1997**, *109*, 130; *Angew. Chem., Int. Ed. Engl.* **1997**, *36*, 156. Dunitz, J. D.; Taylor, R. *Chem. Eur. J.* **1997**, *3*, 89. Reviews: Richmond, T. G. *Coord. Chem. Rev.* **1990**, *105*, 221. Kulawiec, R. J.; Crabtree, R. H. *Coord. Chem. Rev.* **1990**, *99*, 89. Beck, W.; Sünkel, K. *Chem. Rev.* **1988**, *88*, 1405.

(16) Karl, J.; Erker, G.; Fröhlich, R. *J. Am. Chem. Soc.* **1997**, *119*, 11165.

(17) Hoffmann, E. G.; Kallweit, R.; Schroth, G.; Seevogel, K.; Stempfle, W.; Wilke, G. *J. Organomet. Chem.* **1975**, *97*, 183.

(18) Erker, G.; Berg, K.; Angermund, K.; Krüger, C. *Organometallics* **1987**, *6*, 2620.

As expected, the allyl automerization reaction (**4** ⇌ ent-**4**) is a rather slow process in toluene solution [**4** (toluene): $\Delta G^{\ddagger}_{m(obs)}$(273 K) = 18.2 ± 0.3 kcal/mol] but shows a drastically decreased activation energy, when it is taking place in the strongly coordinating solvent tetrahydrofuran [**4** (THF): $\Delta G^{\ddagger}_{m(obs)}$(213 K) = 9.5 ± 0.5 kcal/mol]. This enormous rate enhancement is probably due to a pronounced stabilization of the σ-allyl intermediate by THF coordination (i.e., formation of **6**·THF).

Attaching an electron-donating methyl substituent at each of the Cp ligands has a surprising effect on the enantiomerization barrier. The methylcyclopentadienyl ligand certainly stabilizes a zirconocene cation better than the parent Cp ligand.[21] One might, therefore, have predicted that the bis(methylcyclopentadienyl)(allyl)zirconium betaine (**5**) might exhibit a *lower* activation barrier of the (π-allyl)Zr enantiomerization process than the corresponding unsubstituted reference **4**, because the former system should be expected to lead to an electronically better stabilized (σ-allyl)metallocene−betaine intermediate. The experiment shows the opposite effect: in toluene, **5** has a higher enantiomerization barrier [measured, e.g., by ^{1}H NMR equilibration of the diastereotopic (η-$C_5H_4CH_3$) resonances: $\Delta G^{\ddagger}_{m(obs)}$(313 K) = 19.8 kcal/mol], and even in THF, it still seems to be slightly larger at $\Delta G^{\ddagger}_{m(obs)}$(213 K, **5** in THF) = 9.9 kcal/mol. We conclude that other effects (e.g., unfavorable intramolecular steric interaction or steric hindrance of solvation of the respective intermediate **6**) seem to override the expected electronic stabilization of the electron-deficient metallocene cation moieties in these betaine systems.

The allyl automerization process can probably also be used as a monitoring device to answer the question about the reason why most disubstituted (or higher substituted) alkenes are not polymerized by most group 4 metallocene Ziegler catalysts.[1] If a reaction scheme analogous to that depicted in Scheme 1 applies, the observed unreactivity of these olefins could either be due to effective hindrance of the primary coordination of these sterically more bulky alkenes or reflect a reluctance of these alkenes to undergo the actual insertion step. This question is easily answered for system **5**, which is an active polymerization catalyst of ethene, propene, and their homologous 1-alkenes but does not catalyze the polymerization of internal or 1,1-disubstituted olefins. We measured the (π-allyl) automerization barrier of the betaine system **5** in toluene solution in the presence of an excess (ca. 5-fold) of the disubstituted alkenes listed in Table 1 and have in all these cases found that the $\Delta G^{\ddagger}_{m(obs)}$ values were within the experimental error undistinguishable from that in pure alkene-free toluene. These disubstituted alkenes apparently do not coordinate to the cationic metal center in the metallocene borate betaine systems. It seems to be hindrance of the first, the coordination step, that renders these 1,1- and 1,2-disubstituted alkenes unsuited for polymerization by the metallocene Ziegler catalyst.

Table 1. Activation Energies of the Degenerate Allyl Inversion Process ($\Delta G^{\ddagger}_{m(obs)}$) of **5** in the Presence of Various Alkenes or Solvents[a]

	T, K	$\Delta G^{\ddagger}_{m(obs)}$
toluene	313	19.8
2-methyl-1-butene	313	19.8
2-methyl-1-pentene	313	19.7
isobutylene	313	19.7
trans-2-butene	298	19.7
cis-2-butene	323	19.6
1-hexene	323	18.9
1-pentene	303	17.7
1-butene	293	17.5
propene	293	17.2
THF	213	9.9

[a] Gibbs activation energies under standard-state conditions ($c^{\ominus}$ = 1 mol L^{-1}) in kcal mol^{-1}; measured in dilute toluene solution (except THF); exchange in all cases followed by Cp−CH_3 exchange, in many cases in addition by allyl 1-H_{syn}/1-H_{anti} exchange in the ^{1}H NMR spectra.

The metallocene borate betaines **5** are very active catalysts for the polymerization of ethene and of α-olefins, as we had recently shown.[14,16] During a rapidly proceeding initiation period, the metallocene and the borate ends of the betaine system become separated by a growing hydrocarbon chain between them. Then chain transfer liberates an oligoalkylene-modified R−B$(C_6F_5)_3^-$ anion (which was positively identified by LDI-TOF-MS)[14,22] and the metallocene cation enters into the cycle of repetitive CC coupling of alkene monomers to give the respective polymers.

The systems **4** and **5** are unique in the sense that they have allowed us to directly observe the first step of, e.g., ethene insertion by NMR spectroscopy.[11b] Under carefully controlled conditions at low temperature, e.g., **5** reacts with the alkene and "rests" after the first insertion step until the next insertion initiates spontaneous chain growth without allowing us to detect and identify further intermediate species so far. The monoinsertion product was identified and characterized as the metallacycle **9** by a combination of NMR spectroscopic methods.[23] A weak coordination of the C4−C5 double bond assisted by an intramolecular Zr···C(6)H_2[B] ion-pair interaction[24] was identified and most probably held responsible for an overall energy gain that just allows us to "see" the product of the very

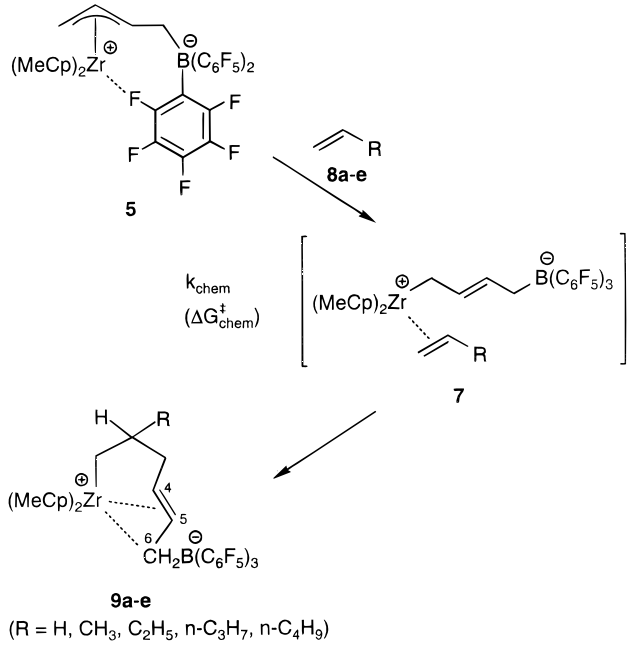

(19) For π-alkene group 4 metallocene cation model systems, see, e.g.: Horton, A. D.; Orpen, A. G. *Organometallics* **1992**, *11*, 8. Wu, Z.; Jordan, R. F.; Petersen, J. L. *J. Am. Chem. Soc.* **1995**, *117*, 5867. Casey, C. P.; Hallenbeck, S. L.; Pollock, D. W.; Landis, C. R. *J. Am. Chem. Soc.* **1995**, *117*, 9770. Galakhov, M. V.; Heinz, G.; Royo, P. *J. Chem. Soc., Chem. Commun.* **1998**, 17. Casey, C. P.; Fagan, M. A.; Hallenbeck, S. L. *Organometallics* **1998**, *17*, 287.

(20) For rare examples of such alkene insertions that were experimentally studied, see, e.g.: Pino, P.; Cioni, P.; Wei, J. *J. Am. Chem. Soc.* **1987**, *109*, 6189. Young, J. R.; Stille, J. R. *J. Am. Chem. Soc.* **1992**, *114*, 4936. Yang, X.; Jia, L.; Marks, T. J. *J. Am. Chem. Soc.* **1993**, *115*, 3392. Horton, A. D. *Organometallics* **1996**, *15*, 2675. Casey, C. P.; Hallenbeck, S. L.; Wright, J. M.; Landis, C. R. *J. Am. Chem. Soc.* **1997**, *119*, 9680.

(21) Gassman, P. G.; Callstrom, M. R. *J. Am. Chem. Soc.* **1987**, *109*, 7875. Gassman, P. G.; Mickelson, J. W.; Sowa, J. R., Jr. *J. Am. Chem. Soc.* **1992**, *114*, 6942.

first alkene insertion step. This unique feature of, e.g., the **5** plus 1-alkene catalyst system has opened a possibility to gain some quantitative information about the activation parameters of the alkene insertion reaction at the active metallocene catalyst center and to arrive at a good qualitative estimate of the Gibbs activation energy of the essential carbon−carbon coupling step.

An experimental complication arose from the fact that only a rather small "temperature window" allowed the observation of the formation of the primary insertion products **9** under

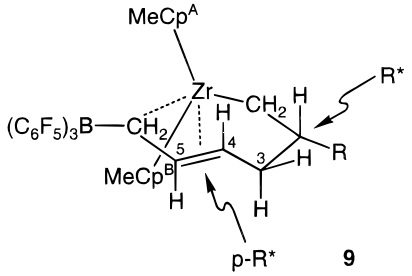

kinetically clean conditions. It usually required a specific temperature (T_{obs}, see below) to monitor product formation by ^{1}H NMR spectroscopy at a reasonable rate, and mostly the system was getting kinetically complicated at only a slightly higher temperature due to the onset of the massive polymerization reaction. It turned out that the overall situation was best for the bis(methylcyclopentadienyl)zirconium-derived systems, where a clean "kinetic temperature window" of ca. 15−20 °C was pertained. We, therefore, limited this study to employing the $(MeCp)_2Zr(\mu\text{-}C_4H_6)B(C_6F_5)_3$ betaine system **5** as a starting material and can at present reliably report only Gibbs activation energy data ($\Delta G^{\ddagger}$), although having the respective enthalpic ($\Delta H^{\ddagger}$) and entropic contributions of the activation barriers in question would be highly desirable and their reliable experimental determination should be attempted in the future.

The $(MeCp)_2Zr(\mu\text{-}C_4H_6)B(C_6F_5)_3$ system **5** cleanly adds 1 equiv of propene at −20 °C to yield a single diastereomeric propene insertion product (**9b**, R = CH_3). We assume that it is characterized by a pseudoequatorial positioning of the CH_3 substituent at the crown-shaped metallacyclic ring system.[23] In addition, the betaine **5** was reacted with the α-alkenes 1-butene, 1-pentene, and 1-hexene, respectively. In all these cases, the reactions proceed more slowly with increasing length of the 1-alkenyl chain but, in all cases, result in a clean formation of a single chiral metallacyclic insertion product. Regiochemical control is perfect. Within the limits of detection, only the [1,2] insertion products are formed, i.e., the R group originating from the incoming alkene ends up in the β-position at the metallacyclic framework of **9**. Stereocontrol is equally pronounced;

Scheme 2

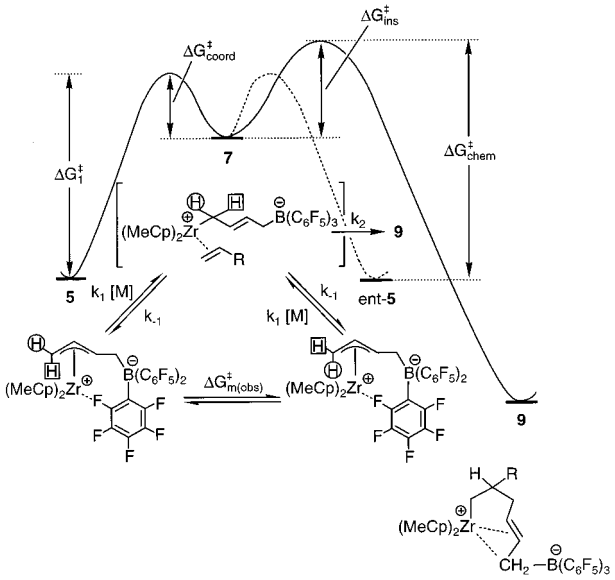

in all these examples of complexes **9** formed in this study, it must be assumed that a *relative* 2-*R**,3-5-*p*-*R** product configuration is attained, probably resulting in the least steric hindrance.

The formation of the products **9b**−**e** was specifically investigated in this study. The products **9b**−**e** were prepared directly in toluene-d_8 solution. They are rather fragile compounds that were not isolated but thoroughly characterized by a combination of ^{1}H and ^{13}C NMR methods (analogously as described previously for **9a**).[23] The 1-hexene insertion product (**9e**) may serve as a typical example. Complex **9e** was prepared by treatment of the betaine **5** with 1-hexene for 15 h at −15 °C in toluene-d_8. The metallacycle **9e** is characterized by the presence of a pair of diastereotopic MeCp ligands (eight methine ^{1}H/^{13}C NMR signals at δ 5.46, 5.26, 5.16 (2H), 5.11 (2H), 5.04, 4.76/116.9, 114.7, 114.5, 111.6, 110.3, 109.2, 109.0, 107.2 ppm and a corresponding pair of methyl resonances at δ 1.46, 1.24/14.6, 14.5 ppm). The ^{13}C NMR signals of the ring carbon atoms of complex **9e** appear at δ 58.0 (C1), 54.1 (C2), 41.5 (C3), 141.3 (C4), 125.4 (C5), and ca. 7 (br, C6). The NMR chemical shifts of the latter three ^{13}C carbon resonances (by comparison with the respective literature values of the **9a**/**9a**·THF references) clearly indicate coordination of all three carbon centers of the terminal $-C^4H{=}C^5HC^6H_2$[B] moiety to zirconium. As expected, diastereotopic methylene hydrogen atoms were observed of the C^1H_2 (δ −0.55, ca. 0.9), C^3H_2 (δ 0.69, 1.48), and C^6H_2 (δ 0.28, 0.49) moieties. The diastereotopic differentiation is also observed for the three methylene groups of the 1-hexene-derived *n*-butyl substituent that is attached at the metallacyclic C2 position (C^7H_2, δ 0.70, ca. 0.9; C^8H_2, δ 0.88, 1.05; C^9H_2, δ 1.22, 1.86). Complex **9e** exhibits three sharp ^{19}F resonances of the $B(C_6F_5)_3$ unit (δ −165.9 (m), −160.8 (p), −133.5 (o) at 253 K in toluene-d_8). There is no indication of any residual zirconium-to-fluorine interaction in the products **9**.

The second-order rate constant (k_{chem}; corresponding to $\Delta G^{\ddagger}_{chem}$ in Scheme 2) of the first insertion of propene into the Zr−C bond of **5** was determined in the following way. The betaine **5** was prepared in situ from $(MeCp)_2Zr$(butadiene) and $B(C_6F_5)_3$ in toluene-d_8. A measured amount of ferrocene was added as an internal standard for ^{1}H NMR integration. At −40 °C, ca. 6 mL of gaseous propene was passed into the solution, which resulted in a condensation of a large enough quantity of the α-olefin to allow for a determination of k_1 under pseudo-

(22) Karl, J. Doctoral dissertation, Münster, 1997.

(23) Temme, B.; Karl, J.; Erker, G. *Chem. Eur. J.* **1996**, *2*, 919. Karl, J.; Erker, G. *J. Mol. Catal.* **1998**, *128*, 85. Karl, J.; Erker, G. *Chem. Ber.* **1997**, *130*, 1261.

(24) For related examples of such ion pair interaction, see, e.g.: Eisch, J. J.; Caldwell, K. R.; Werner, S.; Krüger, C. *Organometallics* **1991**, *10*, 3417. Bochmann, M.; Lancaster, S. J.; Hursthouse, M. B.; Malik, K. M. A. *Organometallics* **1994**, *13*, 2235. Deck, P. A.; Marks, T. J. *J. Am. Chem. Soc.* **1995**, *117*, 6128. Giardello, M. A.; Eisen, M.; Stern, C. L.; Marks, T. J. *J. Am. Chem. Soc.* **1995**, *117*, 12114. Chen, Y.-X.; Marks, T. J. *Organometallics* **1997**, *16*, 3649. Karl, J.; Erker, G.; Fröhlich, R.; Zippel, F.; Bickelhaupt, F.; Schreuder Goedheijt, Akkerman, O. S.; Binger, P.; Stannek, J. *Angew. Chem.* **1997**, *109*, 2914; *Angew. Chem., Int. Ed. Engl.* **1997**, *36*, 2771. Schottek, J.; Erker, G.; Fröhlich, R. *Angew. Chem.* **1997**, *109*, 2585; *Angew. Chem., Int. Ed. Engl.* **1997**, *36*, 2475. Pindado, G. J.; Thornton-Pett, M.; Bochmann, M. *J. Chem. Soc., Dalton Trans.* **1997**, 3115 and references cited in these articles.

Table 2. Characterization of the Essential Rate Constants and Gibbs Activation Energies Involved in the 1-Alkene Insertion Reactions of **5** To Give **9**

alkene	*T*, K	*c*(alkene)[a]	$k_{m(obs)}$[b]	k_{chem}[c]	$\Delta G^{\ddagger}_{chem}$[d]	k_1[c]	Δ	$\Delta G^{\ddagger}_1$[d]	$\Delta\Delta G^{\ddagger}_2$[e]
propene	293	0.035	1.5171	0.7949	17.3	3.4828	0.2957	16.4	0.7
1-butene	293	0.088	0.5193	0.1084	18.5	1.0956	0.1098	17.1	1.3
	293	0.100	0.5690	0.1084	18.5	1.1948	0.0998	17.1	1.3
1-pentene	293	0.064	0.3063	0.0596	18.8	0.6438	0.1020	17.4	1.3
	303	0.051	1.0863	0.1653	18.8	2.2584	0.079	17.3	1.5
	313	0.037	3.0649	0.4636	18.8	6.3704	0.785	17.2	1.6
1-hexene	313	0.061	0.4393	0.0626	20.1	0.9110	0.0738	18.4	1.6
	323	0.061	1.0639	0.1754	20.1	2.2191	0.0858	18.5	1.6

[a] In mol/L in toluene. [b] $k_{m(exp)}/c$(alkene) [L/(mol·s)]. [c] $k_{c(exp)}/c$(alkene) [L/mol·s]. [d] In kcal/mol, calculated for $c^{\ominus} = 1$ mol L^{-1} standard state. [e] Obtained from the calculated $\Delta(=k_2/k_{-1})$ value (for definitions, see Scheme 2).

first-order conditions. The sample was brought to the reaction temperature of 253 K inside the probe of a 600-MHz NMR spectrometer, and the progress of the reaction was monitored at 1-min intervals by integration of the well-separated $C_5H_4CH_3$ signals of the starting material. At an alkene concentration of *c*(propene) = 0.096 mol/L, a rate constant of $k_{chem} = 6.30 \times 10^{-3}$ L mol^{-1} s^{-1} was derived (see Experimental Section).

The analogous insertion reaction of 1-butene into the Zr−C bond of **5** is markedly slower. Under otherwise similar conditions, we had to increase the reaction temperature to 273 K to obtain a rate constant of $k_{chem} = 9.93 \times 10^{-3}$ L mol^{-1} s^{-1}. 1-Pentene is even more slowly inserted ($k_{chem} = 4.79 \times 10^{-3}$ L mol^{-1} s^{-1}), and 1-hexene inserts even slower into **5** ($k_{chem} = 6.26 \times 10^{-2}$ L mol^{-1} s^{-1} at 313 K). For the purpose of comparison, the respective Gibbs activation energies ($\Delta G^{\ddagger}_{chem}$) were calculated for these reactions at standard state conditions ($c^{\ominus} = 1$ mol L^{-1}).[25] This revealed a steady increase of the overall activation barrier of the formation of the first insertion products **9b**−**e** (starting from **5**) on going from propene ($\Delta G^{\ddagger}_{chem}$(253 K) = 17.3 kcal/mol) to 1-butene ($\Delta G^{\ddagger}_{chem}$(273 K) = 18.5 kcal/mol), 1-pentene ($\Delta G^{\ddagger}_{chem}$(273 K) = 18.8 kcal/mol), and 1-hexene ($\Delta G^{\ddagger}_{chem}$(313 K) = 20.1 kcal/mol). This corresponds to the order of reactivity of 1-alkenes at typical metallocene Ziegler catalyst systems, where a decrease of the reaction rate with increasing lengths of the 1-alkene substituent is also observed.

The rate of the dynamic allyl inversion process ($k_{m(obs)}$) of the metallocene−betaine starting material **5** is markedly increased in the presence of these reactive 1-alkenes. The more reactive the 1-alkene is with regard to the insertion reaction, the stronger is its acceleration effect on the **5** ⇌ ent-**5** automerization reaction (as measured by temperature-dependent ^{1}H NMR spectroscopy). 1-Hexene in toluene solution results in a decrease of the $\Delta G^{\ddagger}_{m(obs)}$ activation barrier of **5** by about 1 kcal/mol (from 19.8 kcal /mol in pure toluene solvent to 18.9 kcal/mol), whereas a barrier of $\Delta G^{\ddagger}_{m(obs)} = 17.2$ kcal/mol is eventually monitored in the presence of the more reactive propene. This rate acceleration effect presumably results from a stabilization of the (*σ*-allyl)metallocene−betaine intermediate by the added alkene, i.e., the formation of the (*σ*-allyl)(*π*-1-alkene)metallocene intermediate **7** (see Scheme 2).

We note that the activation energy of the overall chemical reaction ($\Delta G^{\ddagger}_{chem}$) is apparently in the same order of magnitude as the Gibbs activation energy ($\Delta G^{\ddagger}_{m(obs)}$) of the allyl automerization process of the starting material **5** in the presence of reactive 1-alkenes, as was determined by dynamic NMR spectroscopy (see above and Table 1). It is very reasonable to assume that both these reactions proceed through the same type of intermediate, namely, an (*σ*-allyl)metallocene betaine. We must even assume that the identical intermediate, the (*σ*-allyl)-metallocene olefin complex **7(b**−**e)** is the essential intermediate stage for both the chemical insertion reaction (k_{chem}, leading to **9**) and the allyl inversion reaction ($k_{m(obs)}$, leading to $MeCp^A$/$MeCp^B$ and allyl-1-H_{syn}/1-H_{anti} equilibration, respectively, on the NMR time scale). The rate constants k_{chem} and $k_{m(obs)}$ being in the same range, however, means that these two reactions are no longer independent of each other. This is readily illustrated if a selection of limiting kinetic situations is assumed for such a situation of these two competing reaction branches as is depicted in Scheme 2. Let us assume that the reaction follows the pathway starting from **5** along the reaction coordinate as illustrated in Scheme 2. *π*-Allyl to *σ*-allyl conversion in combination with olefin coordination brings the system across the first barrier to the stage of the essential (*σ*-allyl)(olefin)-metallocene betaine intermediate **7**. This can then either react back (k_{-1})—which we would not notice[26]—or simply follow the symmetry equivalent k_{-1} pathway (dotted line in Scheme 2) to the allyl inverted product ent-**5**. This reaction branch is quantitatively monitored by the dynamic NMR experiment (see above). With a reactive alkene coordinated to the metal center, the intermediate **7** will, however, competitively undergo irreversible chemical insertion of the alkene (k_2) with the k_{-1} pathways to form the insertion product **9**. If the k_2 pathway is rapid, it will successfully deviate a sizable quantity of the intermediate **7** from the allyl inversion pathway and, thereby, directly lead to an increase of the *apparent* activation barrier of the allyl inversion NMR experiment (decrease of $k_{m(obs)}$). In the extreme situation with a large difference of these two rate constants ($k_{-1}/k_2 \rightarrow 0$), the allyl enantiomerization process of the starting material will no longer be experimentally observed at all. On the other hand, the limiting maximum $k_{m(obs)}$ value can, in the presence of an insertion-active alkene, only be expected to be measured experimentally (by dynamic NMR spectroscopy) in an extreme situation when the insertion rate (k_2) is much smaller than k_{-1}.

In the given situation with rather insertion-reactive 1-alkenes being added, we will, in fact, measure an *apparently* decreased actually observed NMR rate constant ($k_{m(obs)}$) of the allyl inversion process of **5** under these circumstances (see Tables 1 and 2) relatively to the possible limiting value (k_1).

This interesting competition situation between degenerate (allyl)metallocene inversion and alkene insertion can be used to experimentally determine the magnitude of the **5** → **7** barrier (k_1; $\Delta G^{\ddagger}_1$) and its difference to the second barrier (k_2/k_{-1}; $\Delta\Delta G^{\ddagger}_2$; see Chart 1) by connecting the rate expression of the observed magnetization transfer

(25) Moore, J. W.; Pearson, R. G. *Kinetics and Mechanism*; Wiley: New York, 1981; pp 178−181. Robinson, P. J. *J. Chem. Educ.* **1978**, *55*, 509.

(26) Green, M. L. H.; Wong, L.-L.; Seela, A. *Organometallics* **1992**, *11*, 2660 and references cited therein.

Chart 1

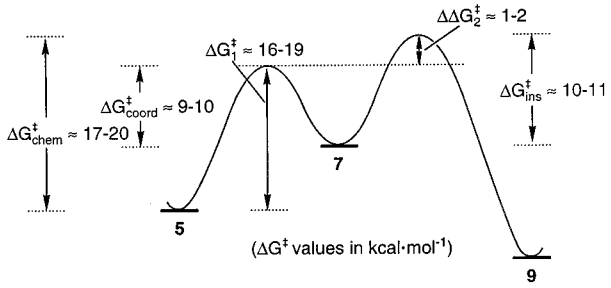

$$\frac{\mathrm{d}[\text{ent-}\mathbf{5}]}{\mathrm{d}t} = k_{\mathrm{m(obs)}}[\mathbf{5}][\mathrm{M}] = k_{-1}[\mathbf{7}] \tag{2}$$

and the rate law of the chemical reaction **5** → **9**

$$-\frac{\mathrm{d}[\mathbf{5}]}{\mathrm{d}t} = k_1[\mathbf{5}][\mathrm{M}] - k_{-1}[\mathbf{7}] = k_{\mathrm{chem}}[\mathbf{5}][\mathrm{M}] \tag{3}$$

with the steady-state expression of the proposed intermediate **7**.

$$\frac{\mathrm{d}[\mathbf{7}]}{\mathrm{d}t} = k_1[\mathbf{5}][\mathrm{M}] - 2k_{-1}[\mathbf{7}] - k_2[\mathbf{7}] = 0 \tag{4}$$

This leads to the simple rate equations

$$k_{\mathrm{m(obs)}} = \frac{k_1}{2 + \Delta} \tag{5}$$

and

$$k_{\mathrm{chem}} = k_1 - \frac{k_1}{1 + \Delta} \tag{6}$$

with

$$\Delta = \frac{k_2}{k_{-1}}$$

Since the rate constants k_{chem} and $k_{\mathrm{m(obs)}}$ can be determined directly by kinetically following the **5** plus alkene → **9** reaction and the alkene-dependent $\mathrm{MeCp^A/MeCp^B}$ or the allyl-1-H_{syn}/1-H_{anti} magnetic exchange of **5**, respectively, the two equations (5) and (6) combined determine k_1 and k_2/k_{-1} directly; namely,

$$k_1 = \frac{2k_{\mathrm{m(obs)}} + k_{\mathrm{chem}}}{2} + \left[\left(\frac{2k_{\mathrm{m(obs)}} + k_{\mathrm{chem}}}{2}\right)^2 - k_{\mathrm{m(obs)}}k_{\mathrm{chem}}\right]^{1/2} \tag{7}$$

and

$$\Delta = \frac{k_2}{k_{-1}} = \frac{k_1}{k_{\mathrm{m(obs)}}} - 2 \tag{8}$$

Experimentally, k_{chem} was determined conventionally by following the decrease of [**5**] in the presence of the respective alkene (see above). The apparent rate constant of magnetic $\mathrm{MeCp^A/MeCp^B}$ and allyl-1-H_{syn}/1-H_{anti} NMR exchange of **5** in the presence of the respective alkene was determined using the method originally described by Forsén and Hoffman using a 1D NMR saturation exchange experiment.[27] The saturation experiment was chosen since it allows us to determine the exchange rate constant at a temperature where the exchange is slow on the NMR time scale. For the system **5**, this means that we observe a set of diastereotopic MeCp and allyl-1-H_{syn}/1-H_{anti} ^{1}H NMR signals in the presence of the reactive 1-alkene (propene, butene, pentene, or hexene) at or close to a temperature where the chemical reaction between this starting material and the α-olefin to give the respective monoinsertion product **9**(**b**−**e**) takes place at a reasonable rate. If we name the two respective diastereotopic NMR sites A and A_{inv}, then the two exchanging sites are characterized by the lifetimes τ_A and τ_{Ainv}. Due to the exchange, longitudinal magnetization arrives at site A at M_{zAinv}/τ_{Ainv} and leaves at the rate $-M_{zA}/\tau_A$. Introduction into the Bloch equation[28] leads to

$$\frac{\mathrm{d}M_{zA}}{\mathrm{d}t} = \frac{M_{zA} - M_{0A}}{T_{1A}} + \frac{M_{zAinv}}{\tau_{Ainv}} - \frac{M_{zA}}{\tau_A} \tag{9}$$

and subsequently after integration from $t = 0$ to $t \rightarrow \infty$

$$\frac{1}{\tau_A} = k_A = \frac{M_{0A} - M_{0A\infty}}{M_{zA\infty}T_{1A}} \tag{10}$$

with M_{0A} denoting the magnetization of site A without irradiation of the corresponding site A_{inv}, $M_{zA\infty}$ denoting the magnetization of site A under irradiation of A_{inv} (irradiation time $t \rightarrow \infty$), and T_{1A} denoting the longitudinal relaxation time of site A.

Thus, by, e.g., experimentally determining the relative magnetization transfer between the diastereotopic $C_5H_4CH_3$ ^{1}H NMR resonances and their relaxation times, we have determined the experimental rate constant of exchange ($k_{\mathrm{m(exp)}}$) of **5** at the actual alkene insertion conditions (see Table 2).[29] The value of $k_{\mathrm{m(exp)}}$ is concentration dependent. Division by the alkene concentration then gives $k_{\mathrm{m(obs)}}$.

These measurements have clearly revealed the expected effect. Addition of the reactive 1-alkene leads to chemical insertion (k_{chem}) into the Zr−C bond of **5**, and this results in a pronouncedly competitive kinetic situation between the irreversible chemical CC coupling reaction and the reversible allyl automerization process, which is monitored by the dynamic NMR experiment. This has created a unique situation that has made it possible to characterize the relative positions of the two essential transition states of the overall insertion process by experimentally determining the two components that make up the overall chemical rate constant, namely, the alkene addition rate constant k_1 and the ratio of rate constants k_2/k_{-1} that determines the chemical fate of the essential intermediate of this process, the (σ-allyl)(π-alkene)metallocene betaine complex **7**. From the rate constant k_1 and the k_2/k_{-1} rate constant ratio, we have derived the corresponding Gibbs activation parameters $\Delta G^{\ddagger}_1$ and $\Delta\Delta G^{\ddagger}_2$ (see Chart 1). We have thus achieved an effective separation of the overall activation barrier ($\Delta G^{\ddagger}_{\mathrm{chem}}$) into two sections characterizing essentially the first ($\Delta G^{\ddagger}_1$) and the second step ($\Delta\Delta G^{\ddagger}_2$) of the overall two-stage alkene insertion process of an 1-alkene into the Zr−C bond of the reactive group 4 metallocene catalyst precursor and effective catalyst model system **5**.

The obtained values are listed in Table 2. They show that the two saddle points marking the essential transition states on

(27) Forsén, S.; Hoffman, R. A. *J. Chem. Phys.* **1963**, *39*, 2892. Baine, P.; Gerig, J. T.; Stock, A. D. *Org. Magn. Reson.* **1981**, *17*, 41. Martin, M. L.; Delpuech, J.-J.; Martin, G. J. *Practical NMR Spectroscopy*; Heyden: London, 1980; pp 315−321.

(28) Günther, H. *NMR-Spektroskopie*; Thieme: Stuttgart, 1992.

(29) Actually, the **5** ⇌ ent-**5** equilibration should correctly be described by means of a two-term expression, such as $-\mathrm{d}[\mathbf{5}]/\mathrm{d}t = (k_{\mathrm{m(obs)alkene}}[\mathbf{5}][\mathrm{alkene}])_{\mathrm{alkene}} + (k_{\mathrm{m(obs)solv.}}[\mathbf{5}][\mathrm{solvent}])_{\mathrm{solv}}$. However, the cases encountered here correspond to either of the two limiting situations where the first or the second term can be neglected, respectively.

the group 4 metallocene betaine 1-alkene insertion hypersurface are very close in absolute energies (see Chart 1). In all four cases investigated in this study, i.e., the reactions of **5** with the reactive 1-alkenes propene, 1-butene, 1-pentene, and 1-hexene, the insertion transition state that must be passed as the second barrier on the way to the final CC-coupled products is slightly higher than the initial alkene coordination barrier (see Table 2).[30]

It remains to be determined how deep the energy well is in which the reactive (alkyl)(π-alkene)metallocene intermediate **7** is located and protected from either of its likely reaction modes, the conversion back to the starting material **5** by decomplexation of the added 1-alkene ($\Delta G^{\ddagger}_{coord}$) and the alkene insertion reaction ($\Delta G^{\ddagger}_{ins}$) leading to the CC-coupled product **9**. In principle, solving this problem would require a direct experimental observation of the **5** ⇌ **7** equilibration, but this could not be achieved due to the very unfavorable equilibrium state [$\Delta\Delta G_0$-(**5**−**7**) ≈ 8−11 kcal mol^{-1}; see Chart 1]. Therefore, we sought for a reliable, close model system to achieve at least a good estimate of the relative position of the intermediate **7** on this energy surface. Going from **7** back to **5** requires dissociation of the alkene ligand and a σ-allyl- to π-allyl ligand conversion at zirconium. The experimental determination of the activation energy of the latter isomerization process may become accessible if care is taken that the rearrangement can be followed in an energetically degenerate situation. Bis(allyl)zirconocene (**10**)[31] appears to offer such a possibility. Complex **10** contains a σ-allyl and a π-allyl ligand at the Cp_2Zr unit in a rapidly equilibrating situation. A dynamic process, very fast on the NMR time scale,[18] takes place in **10** that is characterized by a

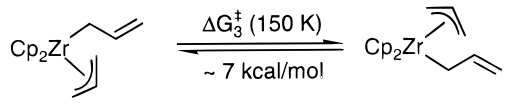

10

σ-allyl to π-allyl ligand conversion that is coupled with the reverse transformation of the other allyl moiety, namely, its π-allyl to σ-allyl interconversion. A Gibbs activation energy of $\Delta G^{\ddagger}_3 \approx 7$ kcal mol^{-1} was measured by dynamic ^{1}H NMR spectroscopy in a $CDFCl_2/CDF_2Cl$ solvent mixture[32] at 150 K. This value may serve as a good first estimate of the energetic σ-allyl to π-allyl interconversion component of the **7** → **5** activation barrier.

It remains to arrive at a quantitative measure of the energetic stabilization of the intermediates **7** arising from the 1-alkene π-coordination. We suggest that the difference between $\Delta G^{\ddagger}_{m(obs)}$ in toluene (19.8 kcal mol^{-1}) and the respective $\Delta G^{\ddagger}_1$ values provides a suitable estimate of the energetic stabilization of the electron-deficient zirconocene center in the (σ-allyl)metallocene-type intermediate resulting from such 1-alkene π-coordination.[24,29]

Table 3. Determination of $\Delta G^{\ddagger}_{ins}$ (313 K) from the Reaction of 1-Alkenes with the Metallocene−Borate−Betaine System **5**[a]

inserted monomer	$\Delta\Delta G^{\ddagger}_2$	$\Delta G^{\ddagger}_3$	$\Delta G^{\ddagger}_{m(obs)}$[b]	$\Delta G^{\ddagger}_1$	$\Delta G^{\ddagger}_{ins}$
propene	0.7	∼7	19.8	16.4	∼11.1
1-butene	1.3	∼7	19.8	17.1	∼11.0
1-pentene	1.5	∼7	19.8	17.3	∼11.0
1-hexene	1.6	∼7	19.8	18.4	∼10.0

[a] According to eq 11; $\Delta G^{\ddagger}$ values in kcal mol^{-1}; standard state ($c^{\ominus}$ = L mol l^{-1}). [b] In toluene in the absence of 1-alkenes.

With these values, the relative position of the essential intermediate **7** on the 1-alkene addition/insertion energy surface is determined. Summation of the respective Gibbs activation energies according to eq 11 then gives the intrinsic activation

$$\Delta G^{\ddagger}_{ins} = \Delta\Delta G^{\ddagger}_2 + \Delta G^{\ddagger}_3 + (\Delta G^{\ddagger}_{m(obs)}(\text{in toluene}) - \Delta G^{\ddagger}_1) \quad (11)$$

energy of the insertion step ($\Delta G^{\ddagger}_{ins}$). A complete listing of these $\Delta G^{\ddagger}$ values for the insertion reactions **5** → **9** using the olefins propene, 1-butene, 1-pentene, and 1-hexene is given in Table 3

Conclusion

The metallocene−betaine system **5** is a direct precursor of a very active homogeneous metallocene Ziegler catalyst system for the polymerization of ethene and reactive 1-alkenes. It is unique in a variety of important aspects; among these, it is distinguished by the fact that the product of the first 1-alkene insertion[11b] step can be kinetically isolated from the remaining reaction sequence of the catalytic initiation period.[14,16,22] This specific feature has allowed us to achieve a good estimate of the intrinsic activation energy ($\Delta G^{\ddagger}_{ins}$) of the 1-alkene insertion reaction into the zirconium−carbon bond of such a catalyst system for the case of the bis(methylcyclopentadienyl)zirconium metallocene backbone. The result of this study is that the essential reactive intermediate, an alkyl(π-1-alkene)metallocene cation type species, is located in a rather deep energy well along the reaction coordinate. The insertion barrier itself seems to be rather independent of the 1-alkene employed (in the propene to 1-hexene homologous series). The $\Delta G^{\ddagger}_{ins}$ activation barrier is ca. 10−11 kcal mol^{-1}. The insertion reaction itself represents the highest barrier along the reaction coordinate followed here (**5** → **7** → **9**). The barrier of alkene decomplexation (i.e., the reverse reaction **7** → **5**) is lower by ca. 1−2 kcal mol^{-1}.

The specific quantitative appearance of the energy profile of the 1-alkene coordination/insertion reaction at the group 4 bent metallocene cation center, as it emerges from this study, leads to the interesting consequence that it is *a priori* not very clear which of the two steps, namely, 1-alkene coordination or the actual insertion reaction, is essential for, e.g., stereocontrol of the CC coupling reaction. The overall kinetic situation, as it has become evident from this study, can easily result in a typical Curtin−Hammett situation similar to what has been found for other important catalytic processes previously,[33] namely, a situation where a preequilibration in the first step can successfully compete with the second (here carbon−carbon coupling) step of the overall reaction sequence.

(30) The method applied here would also have been suited to detect a product transition state energetically located beneath the first barrier. Situations involving a $\Delta\Delta G^{\ddagger}_2$ range between +2 and −1 kcal mol^{-1} can probably be characterized with a reasonable accuracy by this method.

(31) (a) Martin, H. A.; Lemaire, P. J.; Jellinek, F. *J. Organomet. Chem.* **1968**, *14*, 149. (b) See, e.g., for a comparison: Brauer, D. J.; Krüger, C. *Organometallics* **1982**, *1*, 204. Brauer, D. J.; Krüger, C. *Organometallics* **1982**, *1*, 207. Highcock, W. J.; Mills, R. M.; Spencer, J. L.; Woodward, P. *J. Chem. Soc., Chem. Commun.* **1987**, 128. Larson, E. J.; Van Dort, P. C.; Dailey, J. S.; Lakanen, J. R.; Pederson, L. M.; Silver, M. E.; Huffman, J. C.; Russo, S. O. *Organometallics* **1987**, *6*, 2141. Larson, E. J.; Van Dort, P. C.; Lakanen, J. R.; O'Neill, D. W.; Pederson, L. M.; McCandless, J. J.; Silver, M. E.; Russo, S. O.; Huffman, J. C. *Organometallics* **1988**, *7*, 1183. Hauger, B. E.; Vance, P. J.; Prins, T. J.; Wemple, M. E.; Kort, D. A.; Silver, M. E.; Huffman, J. C. *Inorg. Chim. Acta* **1991**, *187*, 91. Erker, G.; Engel, K.; Dorf, U.; Atwood, J. L.; Hunter, W. E. *Angew. Chem.* **1982**, *94*, 915; *Angew. Chem., Int. Ed. Engl.* **1982**, *21*, 914. Erker, G.; Berg, K.; Krüger, C.; Müller, G.; Angermund, K.; Benn, R.; Schroth, G. *Angew. Chem.* **1984**, *96*, 445; *Angew. Chem., Int. Ed. Engl.* **1984**, *23*, 455. Erker, G. *Angew. Chem.* **1989**, *101*, 411; *Angew. Chem., Int. Ed. Engl.* **1989**, *28*, 397.

(32) Siegel, J. S.; Anet, F. A. L. *J. Org. Chem.* **1988**, *53*, 2629.

(33) Halpern, J. *Science* **1982**, *217*, 401.

The results that we have obtained here by using the achiral metallocene system **5** makes us hopeful that this type of experimental investigation can also be carried out using analytically much more complicated ansa-metallocene-derived betaine systems. Future studies will show whether the characteristics of the reaction profile of the catalytic metallocene alkene insertion processes are uniformly similar to the specific system studied here or if there is a great variability depending on the very metallocene backbone employed. Using the unique features of metallocene (μ-hydrocarbyl) borate betaine systems, such as **5**, seems to offer a suitable tool for an advanced experimental characterization of the reaction courses followed at the important group 4 metallocene Ziegler catalyst systems. Together with the increasingly more accurate results from theoretical investigations, this will rapidly lead to a much better and more detailed understanding of these important, very reactive, and potentially very selective catalyst systems.

Experimental Section

General Remarks. All manipulations involving air-sensitive compounds were carried out under argon in a glovebox or using Schlenk-type glassware. Solvents (including deuterated solvents) were dried and distilled under argon prior to use. Tris(pentafluorophenyl)borane was prepared according to a literature procedure;[13] the synthesis of the bis(methylcyclopentadienyl)(μ-butadiene)$B(C_6F_5)_3$ betaine **5** was previously described.[16] Complex **10** was prepared according to a literature procedure.[31] NMR experiments were performed on a Varian Unity Plus 600 spectrometer (^{1}H, 600 MHz; ^{13}C, 150 MHz; ^{19}F, 564 MHz). Assignments in the ^{1}H and ^{13}C NMR spectra were confirmed through GCOSY (gradient ^{1}H−^{1}H COSY), GHSQC (^{1}H−^{13}C gradient heteronuclear single-bond quantum correlation), and GHMBC (^{1}H−^{13}C gradient heteronuclear multiple-bond correlation) spectra.[34] IR spectra were acquired on a Nicolet 5 DXC Fourier transform IR spectrometer. Melting points were obtained by differential scanning calorimetry (DuPont 910); elemental analyses were determined on a Foss−Heraeus CHN−rapid elemental analyzer.

Generation of 5. In this study, the betaine **5** was usually generated *in situ* by the addition of a solution of bis(methylcyclopentadiene)(η^4-butadiene)zirconium (11.4 mg, 37.5 μmol) in 2 mL of toluene-d_8 to a solution of tris(pentafluorophenyl)borane (19.2 mg, 37.5 μmol) in 1 mL of toluene-d_8. An aliquot of this solution was used for the reaction of **5** with the 1-alkenes and for the kinetic measurements. The betaine **5** was isolated on a preparative scale by dissolving complex **3b** (300 mg, 0.99 mmol) and tris(pentafluorophenyl)borane (550 mg, 1.07 mmol) in 2 mL of toluene. After a reaction time of 3 days, the orange crystalline precipitate of betaine **5** was collected by filtration (yield, 700 mg (78%); melting point, 107 °C). ^{1}H NMR (toluene-d_8, 599.9 MHz, 303 K): δ 5.87 (m, 1H, 2-H), 5.50, 5.31 (m, each 1H), 5.23 (m, 3H), 5.20, 5.13 (m, each 1H, C_5H_4), 4.85 (m, 1H, 3-H), 4.79 (m, 1H, C_5H_4), 2.41 (br d, $^2J_{HH}$ = 17.7 Hz, 1H, 4-H′), 2.17 (dd, $^2J_{HH}$ = 17.7, $^3J_{HH}$ = 5.2 Hz, 1H, 4-H), 1.75 (dd, $^2J_{HH}$ = 5.2, $^3J_{HH}$ = 11.5 Hz, 1H, 1-H′), 1.46 (s, 3H, $C_5H_4CH_3$), 1.44 (m, 1H, 1-H), 1.36 (s, 3H, C_5H_4-CH_3). ^{13}C NMR (toluene-d_8, 150.8 MHz, 303 K): δ 148.3 (d, $^1J_{CF}$ = 251 Hz, *o*-$B(C_6F_5)_3$), 139.0 (d, $^1J_{CF}$ = 264 Hz, *p*-$B(C_6F_5)_3$), 137.3 (d, $^1J_{CF}$ = 253 Hz, *m*-$B(C_6F_5)_3$), 134.6 (CH, C-2), 120.3 (CH, C-3), 125.7 (C, ipso-C of C_5H_4), 118.4 (ipso-C and CH of C_5H_4), 112.8, 111.4, 109.5, 109.4, 109.0, 107.9, 107.5 (each CH, C_5H_4), 53.7 (CH_2, C-1), 26.6 (br CH_2, C-4), 14.3, 14.0 (C_5H_4-CH_3), ipso-C of $B(C_6F_5)_3$ not detected. ^{19}F NMR (toluene-d_8, 564.3 MHz, 303 K): δ −165.9 (t, $^3J_{FF}$ = 21.0 Hz, 6F, *m*-F), −162.0 (t, $^3J_{FF}$ = 21.0 Hz, 3F, *p*-F). Due to the dynamic behavior of betaine **5**, the *o*-F resonances were not detected at 303 K. ^{19}F NMR (toluene-d_8, 564.3 MHz, 193 K): δ −209.9 (br, 1F, *o*-F coordinated), −167.2, −166.6 (each 1F), −165.8 (2F), −164.9, −162.1 (each 1F) (each br, *m*-F), −161.8, −160.5, −159.1 (each br, 1F, *p*-F), −137.0, −134.5, −132.6, −131.4, −127.2 (each br, 1F, *o*-F). Coalescence of the *o*-F is reached at 243 K, $\Delta\nu$ (193 K) = 43647 Hz, $\Delta G^{\ddagger}_{exchange}$ = 8.5 kcal/mol. IR (KBr): $\tilde{\nu}$ 3119, 3092, 2963, 2932, 2870, 1645, 1514, 1458, 1381, 1271, 1082, 978, 812 cm^{-1}. Anal. Calcd for $C_{34}H_{20}BF_{15}Zr\cdot 0.5C_7H_8$: C, 52.28, H, 2.81. Found: C, 52.20, H, 3.09. ^{1}H NMR (THF-d_8, 599.9 MHz, 203 K): δ 6.30 (1H), 6.21, 6.14 (each 2H), 6.06, 5.94, 5.82 (each 1H) (each br, C_5H_4), 5.63 (br, 1H, 3-H), 4.87 (br, 1H, 2-H), 2.83 (br, 1H, 4-H′), 2.00 (s, 3H, $C_5H_4CH_3$), 1.94 (br, 1H, 1-H′), 1.89 (s, 3H, $C_5H_4CH_3$), 1.72 (br, 1H, 1-H), 1.54 (br, 1H, 4-H). ^{13}C NMR (THF-d_8, 150.8 MHz, 203 K): δ 148.7 (d, $^1J_{CF}$ = 240 Hz, *o*-$B(C_6F_5)_3$), 143.7 (CH, C-3), 138.6 (d, $^1J_{CF}$ = 241 Hz, *p*-$B(C_6F_5)_3$), 137.9 (d, $^1J_{CF}$ = 231 Hz, *m*-$B(C_6F_5)_3$), 126.7 (C, *i*-$B(C_6F_5)_3$), 117.5, 116.0, 112.0, 110.8, 109.5, 106.9, 106.4, 106.1 (each CH, C_5H_4), 116.0 (CH, C-2), 45.6 (CH_2, C-1), 33.1 (br CH_2, C-4), 15.1, 14.7 (each CH_3, $C_5H_4CH_3$). ^{19}F NMR (THF-d_8, 564.3 MHz, 299 K): δ −168.1 (t, $^3J_{FF}$ = 21 Hz, 6F, *m*-F), −165.1 (t, $^3J_{FF}$ = 21 Hz, 3F, *p*-F), −134.3 (d, $^3J_{FF}$ = 20 Hz, 6F, *o*-F).

Reaction of 5 with 1-Alkenes. General Procedure. An NMR tube containing a solution of the betaine **5** in toluene-d_8, prepared *in situ* as described above, was placed in a Schlenk flask and cooled to −20 °C. While keeping the NMR tube under an argon atmosphere, 3 mL of the gaseous 1-alkene or, in the case of liquid reagents, of olefin vapor was bubbled through the solution by a capillary. The tube was then sealed, taken out of the Schlenk flask, and kept at −15 °C prior to the NMR measurements. In the cases of **9d** and **9e**, the mixture was allowed to react for 15 h at −15 °C before the NMR spectra were collected. The following atom-numbering scheme was used below: ring carbon C1-(at Zr) − C6(attached to B), followed by C7(substituent at C2) − C10 (in case of **9e**).

Reaction of 5 with Propene: Characterization of 9b. ^{1}H NMR (toluene-d_8, 599.9 MHz, 263 K): δ 5.79 (m, 1H, 4-H), 5.59 (m, 1H, 5-H), 5.43, 5.23, 5.20, 5.17 (each 1H), 5.10 (3H), 4.80 (1H) (each m, C_5H_4), 1.81 (m, 1H, 2-H), 1.45 (s, 3H, $C_5H_4CH_3$), 1.37 (m, 1H, 3-H′), 1.23 (s, 3H, $C_5H_4CH_3$), 1.04 (dd, $^2J_{HH}$ = 13.2, $^3J_{HH}$ = 6.1 Hz, 1H, 1-H′), 0.66 (m, 1H, 3-H), 0.62 (d, $^3J_{HH}$ = 6.6 Hz, 3H, 7-H), 0.42, 0.34 (br, each 1H, 6-H and 6-H′), −0.70 (d, $^2J_{HH}$ = 13.2 Hz, 1H, 1-H). ^{13}C NMR (toluene-d_8, 150.8 MHz, 263 K): δ 148.0 (d, $^1J_{CF}$ = 250 Hz, *o*-$B(C_6F_5)_3$), 141.5 (CH, C-4), 139.3 (d, $^1J_{CF}$ = 252 Hz, *p*-$B(C_6F_5)_3$), 137.3 (d, $^1J_{CF}$ = 250 Hz, *m*-$B(C_6F_5)_3$), 124.4 (CH, C-5), 117.2, 114.4, 114.3, 111.6, 110.0, 109.0, 107.9, 107.6 (each CH, C_5H_4), 61.1 (CH_2, C-1), 48.6 (CH, C-2), 42.0 (CH_2, C-3), 27.6 (CH_3, C-7), 14.2, 14.1 (each CH_3, C_5H_4-CH_3), ≈6 (br CH_2, C-6). The ipso-C resonances of $B(C_6F_5)_3$ and $C_5H_4CH_3$ were not detected. ^{19}F NMR (toluene-d_8, 564.3 MHz, 263 K): δ −165.7 (t, $^3J_{FF}$ = 21 Hz, 6F, *m*-F), −160.7 (t, $^3J_{FF}$ = 21 Hz, 3F, *p*-F), −133.4 (d, $^3J_{FF}$ = 21 Hz, 6F, *o*-F).

Reaction of 5 with 1-Butene: Characterization of 9c. ^{1}H NMR (toluene-d_8, 599.9 MHz, 263 K): δ 5.88 (m, 1H, 4-H), 5.59 (m, 1H, 5-H), 5.44, 5.26, 5.19, 5.17, 5.14, 5.11, 5.07, 4.78 (m, each 1H, C_5H_4), 1.63 (m, 1H, 2-H), 1.49 (m, 1H, 3-H′), 1.45, 1.20 (s, each 3H, $C_5H_4CH_3$), 0.95 (m, 1H, 7-H′), 0.91 (m, 1H, 1-H′), 0.73 (m, 1H, 7-H), 0.66 (m, 1H, 3-H), 0.65 (m, 3H, 8-H), 0.46, 0.30 (br, each 1H, 6-H and 6-H′), −0.57 (d, $^2J_{HH}$ = 13.4 Hz, 1H, 1-H). ^{13}C NMR (toluene-d_8, 150.8 MHz, 263 K): δ 148.4 (d, $^1J_{CF}$ = 250 Hz, *o*-$B(C_6F_5)_3$), 141.7 (CH, C-4), 139.4 (d, $^1J_{CF}$ = 250 Hz, *p*-$B(C_6F_5)_3$), 137.4 (d, $^1J_{CF}$ = 250 Hz, *m*-$B(C_6F_5)_3$), 124.4 (CH, C-5), 117.7, 114.8, 114.6, 111.7, 110.6, 109.9, 109.3, 107.5 (each CH, C_5H_4), 57.7 (CH_2, C-1), 55.5 (CH, C-2), 41.3 (CH_2, C-3), 34.6 (CH_2, C-7), 12.2 (CH_3, C-8), 14.2 ($2CH_3$, $C_5H_4CH_3$). ipso-C resonances of $B(C_6F_5)_3$ and $C_5H_4CH_3$ and the C-6 signal were not detected. ^{19}F NMR (toluene-d_8, 564.3 MHz, 263 K): δ −165.6 (t, $^3J_{FF}$ = 21 Hz, 6F, *m*-F), −160.6 (t, $^3J_{FF}$ = 21 Hz, 3F, *p*-F), −133.1 (d, $^3J_{FF}$ = 21 Hz, 6F, *o*-F).

Reaction of 5 with 1-Pentene: Characterization of 9d. ^{1}H NMR (toluene-d_8, 599.9 MHz, 253 K): δ 5.90 (ddd, $^3J_{HH}$ = 16.0, $^3J_{HH}$ = 12.0, $^3J_{HH}$ = 4.0 Hz, 1H, 4-H), 5.59 (m, 1H, 5-H), 5.45, 5.25 (each 1H), 5.16 (2H), 5.11, 5.09, 5.04, 4.74 (each 1H) (each m, C_5H_4), 1.72 (m, 1H, 2-H), 1.47 (m, 1H, 3-H′), 1.45, 1.23 (s, each 3H, C_5H_4-CH_3), 1.07 (m, 1H, 8-H′), 0.90 (m, 1H, 1-H′), 0.89 (m, 1H, 7-H′), 0.88 (m, 1H, 8-H), 0.85 (dd, $^2J_{HH}$ = 7.4 Hz, 3H, 9-H), 0.70 (m, 1H, 7-H), 0.68 (m, 1H, 3-H), 0.49, 0.26 (br, each 1H, 6-H′ and 6-H), −0.59 (d, $^2J_{HH}$ = 13.2 Hz, 1H, 1-H). ^{13}C NMR (toluene-d_8, 150.8 MHz, 253 K): δ 148.4 (d, $^1J_{CF}$ = 250 Hz, *o*-$B(C_6F_5)_3$), 141.9 (CH, C-4), 139.1 (d, $^1J_{CF}$ = 250 Hz, *p*-$B(C_6F_5)_3$), 137.4 (d, $^1J_{CF}$ = 250 Hz, *m*-$B(C_6F_5)_3$), 126.6 (CH, C-5), 116.9, 114.4, 114.2, 111.6, 110.3, 109.1, 108.8, 107.1 (each

(34) Braun, S.; Kalinowski, H.; Berger S. *100 and More Basic NMR Experiments*; VCH: Weinheim, 1996 and references cited therein.

CH, C_5H_4), 57.9 (CH_2, C-1), 53.9 (CH, C-2), 44.2 (CH_2, C-7), 41.5 (CH_2, C-3), 20.9 (CH_2, C-8), 14.7 (CH_3, C-9), 14.4, 14.2 (each CH_3, $C_5H_4CH_3$). ipso-C resonances of $B(C_6F_5)_3$ and C_5H_4-CH_3 and the C-6 signal were not detected. ^{19}F NMR (toluene-d_8, 564.3 MHz, 253 K): δ −165.7 (t, $^3J_{FF}$ = 21 Hz, 6F, *m*-F), −160.8 (t, $^3J_{FF}$ = 21 Hz, 3F, *p*-F), −133.0 (d, $^3J_{FF}$ = 21 Hz, 6F, *o*-F).

Reaction of 5 with 1-Hexene: Characterization of 9e. ^{1}H NMR (toluene-d_8, 599.9 MHz, 253 K): δ 5.91 (ddd, $^3J_{HH}$ = 16.0, $^3J_{HH}$ = 12.0, $^3J_{HH}$ = 4.1 Hz, 1H, 4-H), 5.60 (m, 1H, 5-H), 5.46, 5.26 (each 1H), 5.16, 5.11 (each 2H), 5.04, 4.76 (each 1H) (each m, C_5H_4), 1.86 (m, 1H, 9-H′), 1.72 (m, 1H, 2-H), 1.48 (m, 1H, 3-H′), 1.46, 1.24 (each s, 3H, $C_5H_4CH_3$), 1.22 (m, 1H, 9-H), 1.05 (m, 1H, 8-H′), 0.93 (dd, 2^3J_{HH} = 7.2 Hz, 3H, 10-H), 0.92 (m, 2H, 1-H′ and 7-H′), 0.88 (m, 1H, 8-H), 0.70 (m, 1H, 7-H), 0.69 (m, 1H, 3-H), 0.49, 0.28 (each br, 1H, 6-H′ and 6-H), −0.55 (d, $^2J_{HH}$ = 13.1 Hz, 1H, 1-H). ^{13}C NMR (toluene-d_8, 150.8 MHz, 253 K): δ 148.4 (d, $^1J_{CF}$ = 250 Hz, *o*-$B(C_6F_5)_3$), 141.3 (CH, C-4), 139.1 (d, $^1J_{CF}$ = 250 Hz, *p*-$B(C_6F_5)_3$), 137.4 (d, $^1J_{CF}$ = 250 Hz, *m*-$B(C_6F_5)_3$), 125.4 (CH, C-5), 116.9, 114.7, 114.5, 111.6, 110.3, 109.2, 109.0, 107.2 (each CH, C_5H_4), 58.0 (CH_2, C-1), 54.1 (CH, C-2), 41.9 (CH_2, C-7), 41.5 (CH_2, C-3), 30.2 (CH_2, C-8), 23.6 (CH_2, C-9), 14.6, 14.5 (each CH_3, C_5H_4-CH_3), 14.3 (CH_3, C-10), ≈7 (CH_2, C-6). ipso-C resonances of $B(C_6F_5)_3$ and $C_5H_4CH_3$ were not detected. ^{19}F NMR (toluene-d_8, 564.3 MHz, 253 K): δ −165.9 (t, $^3J_{FF}$ = 21 Hz, 6F, *m*-F), −160.8 (t, $^3J_{FF}$ = 21 Hz, 3F, *p*-F), −133.5 (d, $^3J_{FF}$ = 21 Hz, 6F, *o*-F).

Kinetic Investigation of the 1-Alkene Insertion into the Zr−C Bond of 5. General Procedure. A solution of the betaine **5** was prepared *in situ* using toluene-d_8 containing an accurate internal ferrocene standard (c(Fc) between 0.1 and 0.2 mol/L). According to the general procedure described above, 6 mL of gaseous or 0.5 mL of liquid 1-alkene was injected into the solution at −40 °C. NMR measurements were immediately carried out by recording one scan (^{1}H) each minute for a period of ca. 40 min. The 1-alkene concentration was determined by integration of one separated olefin signal versus the internal ferrocene standard. The pseudo-first-order rate constant $k_{c(exp)}(T)$ was determined by monitoring the decay of the intensities of $C_5H_4CH_3$ signals of **5** and first-order kinetics regression. The second-order rate constants k_{chem} listed in Table 2 are derived from $k_{c(exp)}/c_{alkene}$ and calculated to the respective temperature by using $\Delta G^{\ddagger}_{chem}$, which was assumed to remain constant within the small temperature range investigated in this study.

Formation of 9b. c(propene) = 0.096 mol/L, T = 253 K, $k_{c(exp)}$ = 6.05 × 10^{-4} s^{-1}, $\Delta G^{\ddagger}_{chem}$ = 17.3 kcal/mol. **9c**: c(1-butene) = 0.081 mol/L, T = 273 K, $k_{c(exp)}$ = 8.04 × 10^{-4} s^{-1}, $\Delta G^{\ddagger}_{chem}$ = 18.4 kcal/mol. **9d**: c(1-pentene) = 0.43 mol/L, T = 273 K, $k_{c(exp)}$ = 2.06 × 10^{-3} s^{-1}, $\Delta G^{\ddagger}_{chem}$ = 18.8 kcal/mol. **9e**: c(1-hexene) = 0.061 mol/L, T = 313 K, $k_{c(exp)}$ = 3.82 × 10^{-3} s^{-1}, $\Delta G^{\ddagger}_{chem}$ = 20.1 kcal/mol.

The monomer concentrations of the solutions used in the dynamic NMR measurements were determined analogously using the internal ferrocene standard. The resulting $k_{m(obs)}$ and $\Delta G^{\ddagger}_{m(obs)}$ values are listed in Tables 2 and 3, respectively; the $k_{m(obs)}$ and k_{chem} values listed in Table 2 were calculated for the given temperatures from the experimental values by assuming that the corresponding Gibbs activation energies $\Delta G^{\ddagger}_{m(obs)}$ and $\Delta G^{\ddagger}_{chem}$ were constant in the small temperature range used here.

Dynamic Behavior of $Cp_2Zr(allyl)_2$ (10) in Solution. The temperature-dependent dynamic ^{1}H NMR spectra of **10** were recorded in $CDFCl_2/CDF_2Cl$, which allowed us to freeze out the coupled σ-allyl ⇌ π-allyl interconversion on the NMR time scale. ^{1}H NMR ($CDFCl_2/CDF_2Cl$, 599.9 MHz, 233 K): δ 5.75 (quin, $^3J_{HH}$ = 11.6 Hz, 2H, allyl CH), 5.52 (s, 10H, Cp), 2.88 (d, $^3J_{HH}$ = 11.6 Hz, 8H, allyl CH_2). ^{1}H NMR ($CDFCl_2/CDF_2Cl$, 599.9 MHz, 133 K): δ 6.27 (br, 1H, σ-allyl ═CH), 5.57, 5.49 (br, each 5H, Cp), 5.29 (br, 1H, π-allyl CH), 4.59 (br d, $^3J_{HH}$ = 15.8 Hz, 1H, σ-allyl ═CH_2), 4.43 (br d, $^3J_{HH}$ = 8.2 Hz, 1H, σ-allyl ═CH_2), 2.94 (br d, $^3J_{HH}$ = 8.7 Hz, 1H, π-allyl CH_2), 2.82, 2.69 (br, each 1H, π-allyl CH_2), 1.74 (br, 2H, σ-allyl CH_2), 1.66 (br d, $^3J_{HH}$ = 13.1 Hz, 1H, π-allyl CH_2). Coalescence of cyclopentadienyl H is reached at ca. 150 K; $\Delta\nu$(138 K) = 50 Hz and $\Delta G^{\ddagger}_3$ (150 K) = 7 ± 0.5 kcal/mol.

Acknowledgment. Financial support from the Fonds der Chemischen Industrie, the Deutsche Forschungsgemeinschaft, and the Ministerium für Wissenschaft und Forschung des Landes Nordrhein-Westfalen is gratefully acknowledged. We thank Prof. V. Leute for helpful discussions.

Supporting Information Available: Details of the NMR measurements and tables of the kinetic data and deviations of the kinetic formulas (8 pages, print/PDF). See any current masthead page for ordering and Internet access instructions.

JA9743809